

Doping dependence of the spatially modulated dynamical spin correlations and the superconducting-transition temperature in $\text{La}_{2-x}\text{Sr}_x\text{CuO}_4$

K. Yamada, C. H. Lee, K. Kurahashi, J. Wada, S. Wakimoto, S. Ueki, H. Kimura, and Y. Endoh
Department of Physics, Tohoku University, Aramaki Aoba, Sendai 980-77, Japan

S. Hosoya

Institute of Inorganic Synthesis, Faculty of Engineering, Yamanashi University, Miyamae-cho 7, Kofu 400, Japan

G. Shirane

Department of Physics, Brookhaven National Laboratory, Upton, New York 11973-5000

R. J. Birgeneau, M. Greven, M. A. Kastner, and Y. J. Kim

Department of Physics, Massachusetts Institute of Technology, Cambridge, Massachusetts 02139

(Received 8 September 1997)

Systematic low-energy neutron-scattering studies have been performed on float-zone-grown single crystals of $\text{La}_{2-x}\text{Sr}_x\text{CuO}_4$ with x extending from zero doping, $x=0$, to the overdoped, weakly superconducting regime, $x=0.25$. For x beyond a critical doping value of $x_c \approx 0.05$ the low-energy spin-fluctuation peak position shifts from $(\frac{1}{2}, \frac{1}{2})$ to $(\frac{1}{2} \pm \delta, \frac{1}{2})$, and $(\frac{1}{2}, \frac{1}{2} \pm \delta)$; x_c also represents the onset concentration for superconductivity. For $0.06 \leq x \leq 0.12$ the incommensurability δ follows approximately the quantitative relation $\delta=x$. However, beyond $x \approx 0.12$ the incommensurability tends to saturate around $\delta \approx 1/8$. The superconducting-transition temperature $T_c(x)$ for stoichiometric samples at a given doping scales linearly with δ up to the optimal doping value of x . The peak momentum width of the spin fluctuations at low energies is small throughout the superconducting concentration region except in the strongly overdoped region. An anomalously small width is observed for $x = \frac{1}{8}$. The incommensurate spatial modulation is found to be robust with respect to pair-breaking effects that lower T_c , such as deoxygenation of the sample or replacement of Cu by Zn.

[S0163-1829(98)10409-5]

I. INTRODUCTION

The interplay between magnetic fluctuations and high- T_c superconductivity is a central feature of the basic physics of the lamellar CuO_2 materials. Neutron scattering, which can detect both spatial and dynamical spin fluctuations, is the most direct experimental technique for studying this interplay.

It is well known that the holes introduced into the CuO_2 layers by replacing La^{3+} with Sr^{2+} in $\text{La}_{2-x}\text{Sr}_x\text{CuO}_4$ destroy the antiferromagnetic long-range order at very small values of x , $x \approx 0.02$. Further increase of the Sr concentration creates a state with dynamical spin correlations, which we call here modulated spin correlations or incommensurate spin fluctuations.¹⁻⁴ At the same time, high- T_c superconductivity appears in $\text{La}_{2-x}\text{Sr}_x\text{CuO}_4$ for x values beyond a critical concentration $x_c \approx 0.05$, and T_c reaches its maximum value of about 38 K around the optimal doping $x_0 \approx 0.15$. Therefore, it is important to study the relationship between the superconductivity and the modulated spin correlations, particularly their doping dependence, spanning the hole concentration between the underdoped and overdoped superconducting regions. Although previous experiments by ourselves and others have established the overall topology of the phase diagram, no systematic studies on single crystals have been performed because of the difficulty in preparing single crystals that are: (i) chemically homogeneous, (ii)

relatively impurity free, (iii) stoichiometric, and (iv) large enough for inelastic neutron scattering studies. Further, no single crystal neutron studies have been reported in the overdoped region.

To-date, the modulated spin correlations in such high quality and well characterized crystals have been studied predominantly for the optimally doped superconducting samples with $x_0 \approx 0.15$. As a result, for $\text{La}_{1.85}\text{Sr}_{0.15}\text{CuO}_4$ an energy gap of ~ 3.5 meV in the spin-fluctuation spectrum reflecting the superconducting gap has been observed by neutron scattering. This, in turn, provides invaluable information about the pairing state.⁵ On the other hand, for the underdoped superconductor no well-defined energy gap has been observed so far. Earlier it was speculated that the reason for the absence of such an energy gap was the effect of the random Sr doping; however, recent work on $\text{La}_2\text{CuO}_{4.055}$ has cast doubt on this explanation.⁶ In addition, for the overdoped superconductor ($x > x_0$) essentially no information has been obtained on the spin fluctuations. Finally, there still exist several competing models for the origin of the spatially modulated spin correlations, including: nesting of the Fermi surface,⁷ stripe ordering of the doped holes^{8,9} and percolation of the cluster spin glass.¹⁰

In order to elucidate all these issues, we have undertaken systematic neutron-scattering measurements on $\text{La}_{2-x}\text{Sr}_x\text{CuO}_4$. In particular, we quantitatively determine how the spatial modulation of the spin correlations develops with x and how the incommensurability correlates with

$T_c(x)$. We report here measurements of the doping dependence of the modulated spin correlations for $\text{La}_{2-x}\text{Sr}_x\text{CuO}_4$ over a wide doping region utilizing a series of identically grown and treated crystals. We also present data on a deoxygenated sample in which the superconductivity is destroyed. The energy dependence of the spin fluctuations will be discussed in detail in a separate paper.¹¹

The format of this paper is as follows: Experimental details on the sample preparation and characterization are described in Sec. II. The results of the neutron-scattering measurements are presented in Sec. III. We interpret in Sec. IV the newly obtained results, which demonstrate the intimate relationship between the incommensurate spin fluctuations and the high- T_c superconductivity. A summary and conclusions are given in Sec. V.

II. SAMPLE CHARACTERIZATION

As noted above, in order to compare the modulated spin correlations for samples with different doping levels, we have attempted to exclude any factors that can introduce relative systematic errors. Identical procedures for crystal growth and post-growth heat treatment have been used. We have utilized the traveling-solvent-floating-zone method for crystal growth, which uses no crucible, and therefore, avoids the resulting contamination. Significant experience with this technique has been accumulated for $\text{La}_{2-x}\text{Sr}_x\text{CuO}_4$ with $x=0$ and 0.15; this has made possible the growth of a series of single crystals with $x=0.00, 0.04, 0.06, 0.08, 0.10, 0.12, 0.15, 0.18,$ and 0.25 .¹²⁻¹⁵ The typical size of the crystals is about $6 \text{ mm} \times 35 \text{ mm}$ ($\sim 1 \text{ cm}^3$), and the mosaic spread is $\sim 0.4^\circ$ full width at half maximum.

All of the Sr-doped crystals, except the $x=0.04$ sample, exhibit bulk superconductivity after the post-growth heat treatment under 1 bar of oxygen gas flow at $T = 900^\circ\text{C}$ for 100 h. The content of Sr in each fully oxygenated sample has been established by the following measurements: the superconducting transition temperature T_c has been determined from the temperature dependence of the diamagnetic signal for the zero-field-cooled sample using a superconducting quantum interference device (SQUID) magnetometer; the lattice constants from pulverized single crystal samples have been measured at room temperature with an x-ray-powder diffractometer; and the structural phase-transition temperature T_s between the high-temperature tetragonal (HTT) and low-temperature orthorhombic LTO phases has been measured by neutron diffraction. Furthermore, the magnitude as well as the temperature dependence of the magnetic susceptibility in the normal state were compared with previous results for powder samples. Figure 1 shows the measured T_c and T_s as functions of x , both of which are in good agreement with previous results. As shown in Fig. 1, samples with $x=0.18$ ($T_c=36 \text{ K}$) and 0.25 ($T_c=15 \text{ K}$) are slightly and highly overdoped, respectively. Figure 2 shows the doping dependence of the c -axis lattice constant, which increases monotonically with Sr doping; this confirms the continuous substitution of the La sites with Sr ions. The curve in the figure is drawn by interpolating between results from powder samples that are fully oxygenated.¹⁶ The excellent agreement of the c -axis lattice constant, which is sensitive to any oxygen deficiency, between single crystal and powder samples

verifies the oxygen stoichiometry of our single crystals.

The values of the averaged Sr concentrations so determined are found to coincide with those measured directly by electron probe microanalysis within the instrumental resolution. Further, we have determined that the gradient in the Sr concentration has a maximum value of $0.002/\text{cm}$ along the crystal rod by measuring the difference in T_c between the top and bottom part of the rod. In addition, we find that the observed broadening of the structural phase transition of the large single crystals can be interpreted as arising from a macroscopic gradient in the Sr concentration. Specifically, for the $x=0.10$ and $x=0.18$ crystals we find that the observed maximum broadening is about 12 K (full width at half maximum of an assumed Gaussian distribution of T_c), and this, in turn is comparable to the difference in T_s of 15 K evaluated from the highest and lowest Sr concentrations in crystal rods 3.5 cm in length. Thus, the Sr concentrations as well as the oxygen stoichiometry of the samples are known quite accurately. Further, we may conclude that the observed rounding of T_s reflects macroscopic, rather than microscopic, Sr inhomogeneities. We note here that the maximum deviation of the Sr concentration from its average value is about 0.0035; this is rather larger than the value of 0.0006 reported for our best sample with $x=0.15$.⁵ However, the fundamental properties of the magnetic fluctuations are not affected by such small differences in the Sr concentration. For example, a well-defined energy gap in the magnetic excitations is observed in the $x=0.18$ sample, which shows a much broader

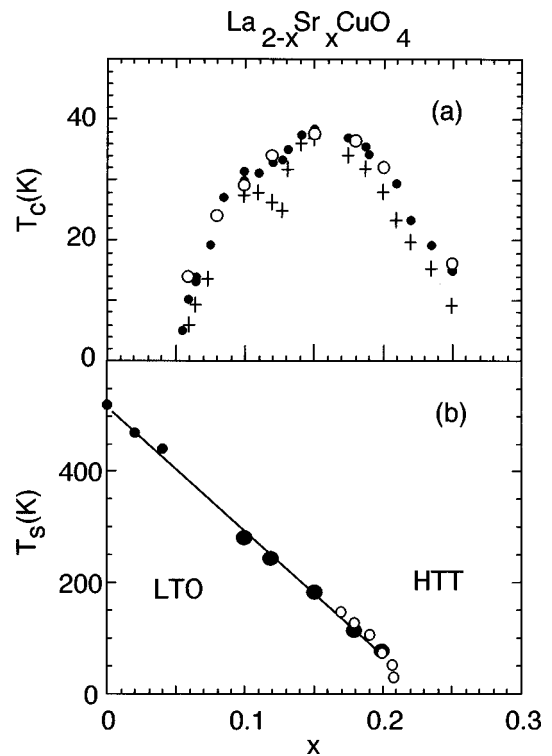


FIG. 1. Sr-doping dependence of (a) superconducting transition temperatures T_c ; onset of T_c [closed circles (Refs. 36 and 37)], open circles (present samples) and midpoint of T_c [crosses (Ref. 36)], (b) structural transition temperatures T_s between the high-temperature tetragonal (HTT) and low-temperature orthorhombic (LTO) phases [open circles (Ref. 36), small closed circles (Ref. 19), large closed circles (present samples)].

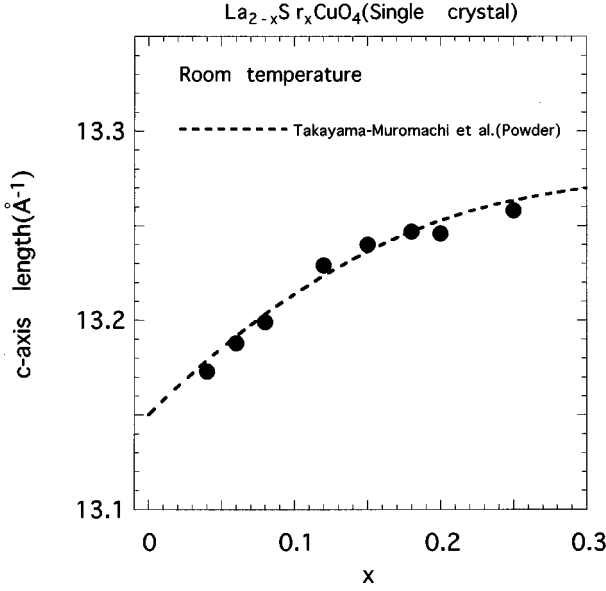


FIG. 2. Lattice constants of $\text{La}_{2-x}\text{Sr}_x\text{CuO}_4$ at room temperature measured on pulverized single crystals by x-ray-powder diffraction (closed circles). The broken curve in the figure is drawn by interpolating results from powder samples (Ref. 16).

transition at T_s than that found in the $x=0.15$ sample.¹¹ Note that the energy gap is only observable for samples near optimal doping, irrespective of any small inhomogeneity of the dopants. This is discussed in detail in Ref. 11.

One single crystal of $\text{La}_{1.85}\text{Sr}_{0.15}\text{CuO}_4$, which initially had $T_c=37.5$ K, has been annealed under Ar gas flow to prepare Sr-doped nonsuperconducting samples. We assume throughout this paper that samples at a given x have their maximum T_c for an exact oxygen stoichiometry of 4.00. The effective doping x_{eff} for annealed $\text{La}_{2-x}\text{Sr}_x\text{CuO}_{4-y}$ is defined as $x-2y$ by assuming that one oxygen ion provides two holes in the CuO_2 planes. We know from previous work that by deoxygenation bulk superconductivity in the optimally doped region disappears for $x_{\text{eff}} \leq 0.11$ due to the reduction of the number of holes and the introduction of the random potential from the oxygen vacancies in the CuO_2 planes.^{17,18} In fact, the superconducting diamagnetic signal of the annealed crystal with x_{eff} smaller than 0.11 is reduced to less than 1% of its original value as shown in Fig. 3. A first annealing has been done at 925 °C, and the resulting decrease of oxygen content is determined to be $y=0.0218 \pm 0.0005$ by weighing the sample before and after deoxygenation with an electrobalance with 10 μg resolution.¹⁸ From this, the effective doping x_{eff} for this deoxygenated sample is found to be 0.106. A second annealing of the deoxygenated crystal at a higher temperature, 950 °C, results in $y=0.0355 \pm 0.0005$, which corresponds to $x_{\text{eff}}=0.079$. It is important to note that the heat treatment controls the oxygen content reversibly; bulk superconductivity reappears when the deoxygenated nonsuperconducting samples are annealed under O_2 gas flow.

III. NEUTRON-SCATTERING EXPERIMENTS AND RESULTS

Inelastic neutron-scattering experiments were performed on the triple-axis spectrometers TOPAN and HER installed

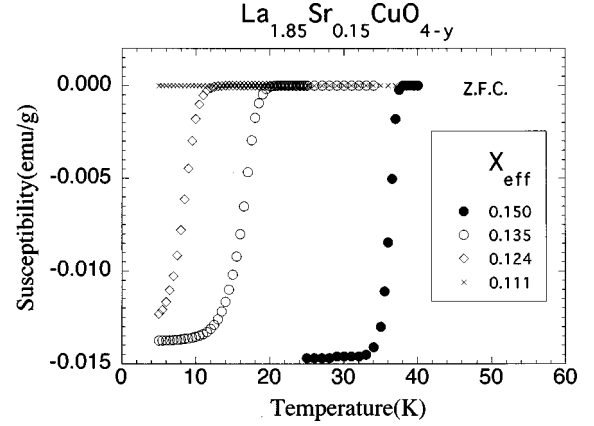


FIG. 3. Diamagnetic susceptibilities measured by a SQUID magnetometer on the zero-field-cooled samples of oxygenated $\text{La}_{1.85}\text{Sr}_{0.15}\text{CuO}_4$ (closed circles) and deoxygenated $\text{La}_{1.85}\text{Sr}_{0.15}\text{CuO}_{4-y}$ samples with various effective doping x_{eff} ($=0.15-2y$).

at thermal and cold neutron beam ports of JRR-3M in JAERI, respectively — TOPAN was used for samples with $x>0.04$ and HER for $x=0$ and 0.04. Vertically focused incident neutrons from a pyrolytic graphite (PG) monochromator with energy 14.7 meV or 4.98 meV were scattered by the sample crystal. A vertically focused PG analyzer then selected scattered neutrons with a specific energy loss caused by the interaction with the spin fluctuations. For the thermal neutron-scattering measurements a pyrolytic graphite filter was used to reduce higher-order neutrons in the incident beam. In addition, a sapphire crystal filter was inserted in between the monochromator and the sample to reduce the high-energy neutron component in the incident neutron flux. For the cold neutron-scattering measurements a cooled Be filter was used to eliminate higher-order neutrons in the incident beam. Additional measurements for single crystals with $x=0.10$ and 0.15 were carried out at the thermal neutron triple-axis spectrometers at the High Flux Beam Reactor at Brookhaven National Laboratory.

The crystals were sealed in an aluminum can filled with He gas for heat exchange. The sample can was attached to the cold plate of a ^4He closed-cycle refrigerator or a pumped ^4He cryostat. The measurements were performed around or below T_c for superconducting samples, and below 7 K for deoxygenated ones. The crystals were aligned with the c axis vertical to the scattering plane. The inelastic magnetic intensities in the $(h,k,0)$ zone of the high-temperature tetragonal phase were monitored by q scans through the positions $(\frac{1}{2}, \frac{1}{2} + \delta, 0)$ and $(\frac{1}{2}, \frac{1}{2} - \delta, 0)$, in contrast to the $(\frac{1}{2}, \frac{1}{2}, 0)$ position that characterizes the commensurate long-range antiferromagnetic order.

Examples of typical q spectra for superconducting $\text{La}_{2-x}\text{Sr}_x\text{CuO}_4$ are shown in Fig. 4. Double peaked signals from the modulated spin correlations are observed in all samples with $0.06 \leq x \leq 0.25$. On the other hand, as will be shown in Fig. 5, commensurate spin fluctuations are observed for the $x=0.04$ sample that is in the so-called semi-conducting spin-glass phase.¹⁹ From the q spectra we extract the two parameters δ and κ_w ; the peak splitting, δ , represents the degree of modulation, or incommensurability, of the spin fluctuations; the peak width, κ_w , defined as the half

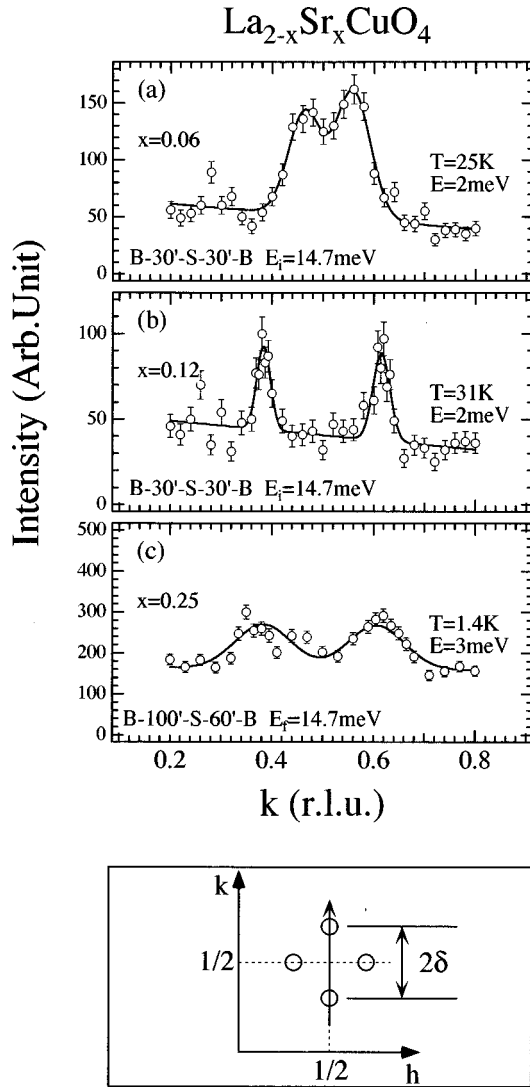


FIG. 4. Inelastic thermal neutron scattering spectra of $\text{La}_{2-x}\text{Sr}_x\text{CuO}_4$ from q scans across the two peaks shown by open circles in the inset; (a) $x=0.06$ at 2 meV, (b) $x=0.12$ at 2 meV, and (c) $x=0.25$ at 3 meV. Note the different experimental condition for $x=0.25$. The solid lines are the results of least squares fitting using two Gaussians plus a flat background. The incommensurability δ is defined as half of the peak splitting between the two peaks at $(\frac{1}{2}, \frac{1}{2} \pm \delta, 0)$ indexed in the tetragonal reciprocal plane $(h, k, 0)$. The position $(\frac{1}{2}, \frac{1}{2}, 0)$ corresponds to an antiferromagnetic Bragg peak position in the long-range-ordered antiferromagnetic phase.

width at half maximum (HWHM) of the peaks, reflects the inverse dynamical coherence length at the measured energy of the spin fluctuations. For the $x=0.25$ sample the peak intensity is significantly weaker than that in the samples with smaller x . Therefore, it is necessary to use coarser instrumental resolution than that employed in the other scans shown in Fig. 4. We note that δ is found to be rather insensitive to the temperature as well as energy transfer up to energies well above ~ 10 meV.²⁰

Figure 5 shows a high-resolution q spectrum for the $x=0.04$ sample obtained by using cold neutrons; an identical q scan for an as-grown sample of La_2CuO_4 is presented in the inset of Fig. 5. It should be noted that the momentum as well as energy resolution in this measurement is better than

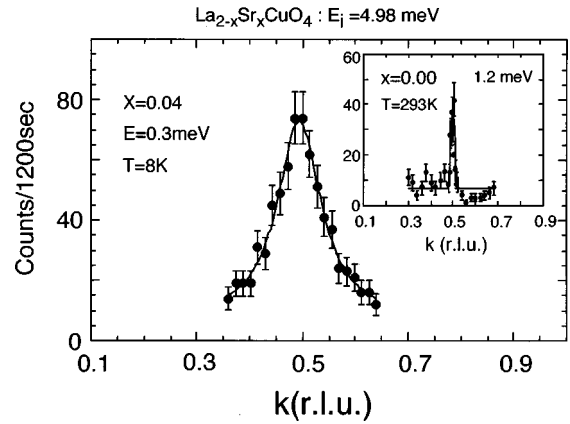


FIG. 5. Inelastic cold neutron-scattering q spectrum of $\text{La}_{2-x}\text{Sr}_x\text{CuO}_4$ for $x=0.04$ at 0.3 meV taken from the same q scan as shown in the inset of Fig. 4(a). The inset shows the q spectrum as-grown La_2CuO_4 at 1.2 meV.

that of the thermal neutron scattering shown in Fig. 4. Although the peak width is much larger than that of the undoped sample (inset of Fig. 5), the spectrum shows a single commensurate peak at $(\frac{1}{2}, \frac{1}{2}, 0)$, as has already been reported in previous thermal neutron-scattering studies on samples with $x=0.02$,^{19,21} 0.03 and 0.04.¹⁹ Therefore, it may be concluded that around $x=0.05$, there exists a phase boundary or crossover region between phases with commensurate and incommensurate spin correlations.

In Fig. 6, we show the doping dependence of κ_w below 3.5 meV around T_c [Fig. 6(a)] and at 8 meV and 8 K [Fig. 6(b)] that are obtained from the q spectra taking into account the instrumental q width. For the nonsuperconducting crystal $x=0.04$, κ_w at 0.4 meV and $T=8$ K is plotted. Within the errors, κ_w depends only weakly on doping in the

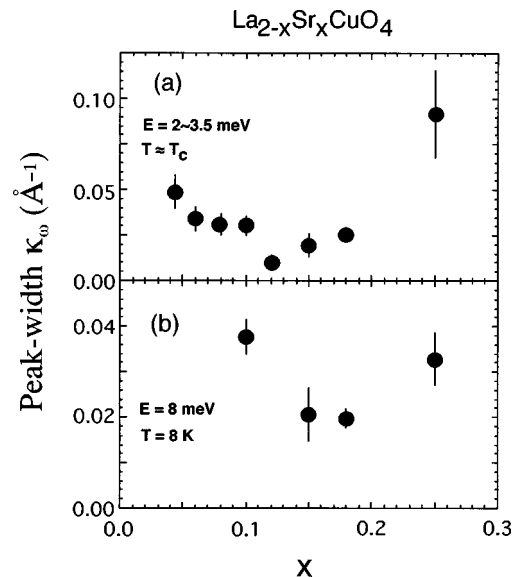


FIG. 6. Sr-doping dependence of the dynamical q width κ_w of the incommensurate peak at (a) $T \approx T_c$ with $E=2-3.5$ meV and (b) below T_c with $E=8$ meV. For the nonsuperconducting sample of $x=0.04$ κ_w at 8 K with $E=0.4$ meV is presented. The instrumental q broadening is removed by least-squares fitting with deconvolution.

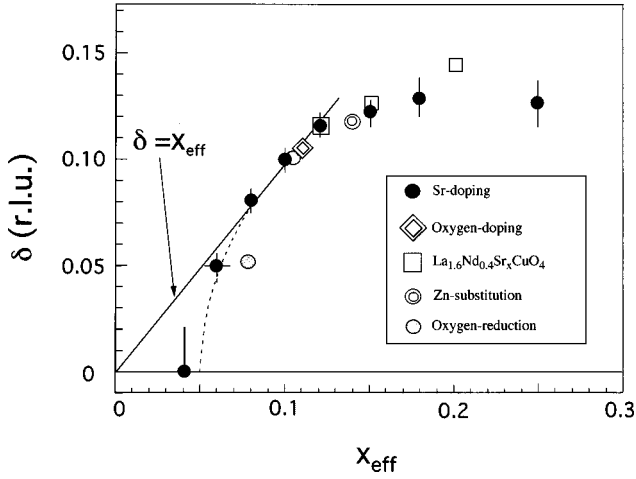


FIG. 7. Sr-doping dependence of the incommensurability δ of the spin fluctuations. The height of the vertical bar at $x=0.04$ indicates the upper limit of δ estimated from the single peaked spectrum in Fig. 5. Data from electrochemically oxygen-doped $\text{La}_2\text{CuO}_{4+y}$ (Ref. 6), $\text{La}_{1.6}\text{Nd}_{0.4}\text{Sr}_x\text{CuO}_4$ (Ref. 38), Zn-substituted $\text{La}_{1.86}\text{Sr}_{0.14}\text{Cu}_{1-y}\text{Zn}_y\text{O}_4$ with $y=0.012$ (Ref. 22) and deoxygenated $\text{La}_{1.85}\text{Sr}_{0.15}\text{CuO}_{4-y}$ (see Fig. 8) are also plotted in the figure.

underdoped and optimally doped regions. However, for $x=0.12$ κ_w is anomalously small; this requires further investigation. We note that, in contrast to κ , κ_w depends sensitively on the fluctuation frequency as well as temperature; the details will be described in a separate paper.¹¹

The incommensurability obtained from fits of two-dimensional Gaussians to the data is plotted in Fig. 7 as a function of x_{eff} . Several characteristics of the doping dependence of the modulated spin correlations can be seen. First, there is a nonlinear relation between the incommensurability δ and the Sr concentration x . The double-peaked structure due to the incommensurate spin fluctuations becomes noticeable with doping only above $x \approx 0.05$, identical, within the uncertainties, with the superconducting phase boundary. For $x > 0.05$, δ increases continuously upon doping, and for $0.06 \leq x < 0.12$, it follows within the errors the quantitative relation, $\delta = x$. Beyond $x \approx 0.12$ the incommensurability δ appears to saturate at the value $\delta \approx \frac{1}{8}$. In the figure, we also plot the results of the deoxygenated samples, which will be described later.

In Fig. 8, we compare the q spectra of the deoxygenated samples $\text{La}_{1.85}\text{Sr}_{0.15}\text{CuO}_{4-y}$ with that of the oxygenated superconducting $x=0.15$ sample (oxygenated samples are presumed to have $y=0$). The incommensurability δ for the deoxygenated $x=0.15$ sample with effective doping level $x_{\text{eff}}=0.106$ is apparently smaller than that for oxygenated $x=0.15$, but similar to that for the oxygenated stoichiometric $x=0.10$ sample as shown in Fig. 7. This result, therefore, indicates that the hole concentration can be changed by changing oxygen content, and that δ is determined by the effective doping level x_{eff} irrespective of the type of dopant. Furthermore, it is important to note that the incommensurability around x_0 is *not* severely altered by pair-breaking effects which destroy the superconductivity. A similar result has been previously obtained for nonsuperconducting $\text{La}_{2-x}\text{Sr}_x\text{Cu}_{1-y}\text{Zn}_y\text{O}_4$ with $x=0.14$ and $y=0.012$, where the doping level was, to first order, unchanged by the Zn ions.²²

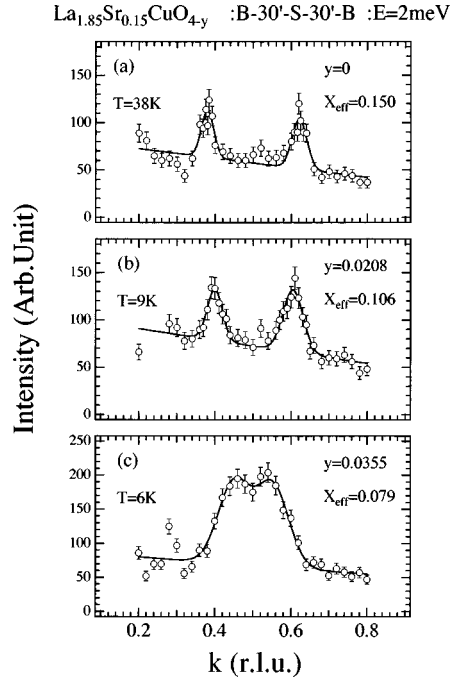


FIG. 8. Inelastic neutron-scattering spectra at 2 meV taken from (a) the superconducting sample with $x=0.15$, and the deoxygenated nonsuperconducting crystal with $x=0.15$ with the effective doping of (b) $x_{\text{eff}}=0.106$ and (c) with $x_{\text{eff}}=0.079$. The δ 's for the deoxygenated samples are shown in Fig. 7 and 9 as a function of x_{eff} .

However, as the deoxygenation is increased (cf. the result for $x_{\text{eff}}=0.079$ in Fig. 4) and the commensurate-incommensurate transition or crossover is approached, the incommensurate state becomes unstable by deoxygenation presumably due to the combined effects of the reduced hole concentration and the random potential of the oxygen vacancies. One should also note the increased broadening of the dynamical q width of the incommensurate peak after deoxygenation of the crystal as shown in Fig. 8.

IV. DISCUSSION

A. Doping dependence of the incommensurability

The doping dependence of δ shown in Fig. 7 should play a central role in distinguishing models for the incommensurate spin fluctuations. However, before attempting any quantitative discussion we must first consider the relation between the number of holes p in the CuO_2 plane and the dopant concentration x . In the systematic study of Torrance *et al.*²³ on ceramics, a linear variation of p with x was observed up to $x_s \approx 0.28$ or 0.36 if the samples were annealed in 1 bar or 100 bars of oxygen pressure, respectively. However, beyond x_s , Torrance *et al.*²³ found that p saturates upon Sr doping due to the introduction of oxygen vacancies. Therefore, on the basis of these results it would seem that the present nonlinear δ - x relation beyond $x \approx 0.12$, and the saturation of δ in the overdoped region up to $x=0.25$, as shown in Fig. 7, is not related to the nonlinear p - x relation due to oxygen vacancies.

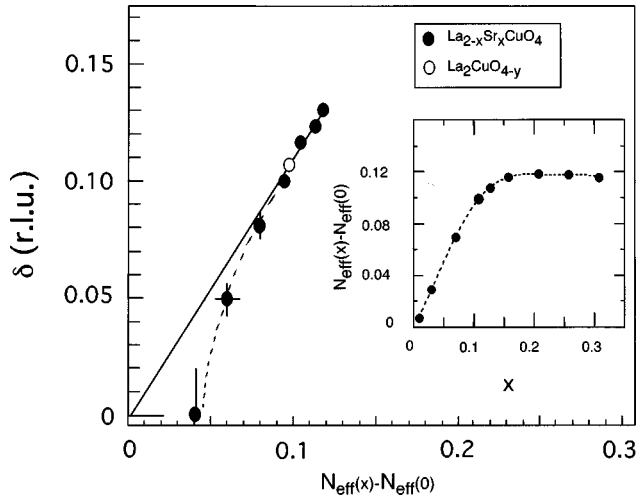


FIG. 9. δ as a function of $N_{\text{eff}}(x) - N_{\text{eff}}(0)$ evaluated from the energy-integrated spectral weight of the optical conductivity within the charge gap of as-grown La_2CuO_4 (see the text for details). The inset shows the Sr-doping dependence of $N_{\text{eff}}(x) - N_{\text{eff}}(0)$ (Ref. 28). $N_{\text{eff}}(x) - N_{\text{eff}}(0)$ is normalized by assuming an $N_{\text{eff}}(x) - N_{\text{eff}}(0) = x$ relation for $x < 0.1$.

In contrast to the above results, even in the doping region below $x=0.25$ several transport experiments suggest a non-linear dependence of carrier number on x , or alternatively, a change in carrier character upon doping beyond x_0 . For example, both the electrical conductivity and the Hall coefficient indicate a crossover in carrier character around the optimal doping x_0 . The expected change in the Fermi surface geometry upon doping from a “small Fermi surface” to a “large Fermi surface” as predicted by several calculations^{24,25} may be connected with such a change in the carrier character. Thus, one possible explanation of the saturation of the incommensurability above $x \approx 0.12$ may be the saturation of the density of $O(2p)$ -type holes. Supporting evidence for this approach comes from the optical measurements of Uchida *et al.*²⁶ They find that N_{eff} , the energy-integrated spectral weight of the optical conductivity within the charge gap of the undoped system, depends on doping x in a manner quite similar to that of δ . Here, N_{eff} represents an energy-dependent effective electron number as is discussed by Uchida *et al.*²⁶ In fact, an excellent linear relation between δ and $N_{\text{eff}}(x) - N_{\text{eff}}(0)$ is obtained as shown in Fig. 9. In the inset, the Sr-doping dependence of $N_{\text{eff}}(x) - N_{\text{eff}}(0)$ integrated up to 1.2 eV is shown.²⁶ We explicitly consider $N_{\text{eff}}(x) - N_{\text{eff}}(0)$ in order to take into account the excess oxygen holes in as-grown samples of La_2CuO_4 at $x=0$. In the figure, δ seems to terminate around 0.12, that is, δ increases linearly with the effective hole concentration up to around $p \approx 0.12$.

One speculative possibility is that the effective density of $O(2p)$ holes saturates because of a change in the carrier type to $\text{Cu}(3d)$ in the overdoped region. $\text{Cu}(3d)$ -type carriers should only have a minor effect on the spatial spin modulation. This observation is based on the fact that commensurate spin ordering is found in electron-doped superconductors for dopings up to $x=0.15$; here the doped carriers are dominantly $\text{Cu}(3d)$ type.²⁷ In addition, as noted previously, replacement of $\text{Cu}(3d)$ ⁹ by $\text{Zn}(3d)$ ¹⁰, in $\text{La}_{2-x}\text{Sr}_x\text{Cu}_{1-y}\text{Zn}_y\text{O}_4$

does not change the incommensurability. We note that the doping dependence of δ is quite different from that of the insulating system $\text{La}_{2-x}\text{Sr}_x\text{NiO}_4$ where δ varies linearly with x up to at least $x \approx \frac{1}{2}$ and a well-defined charge ordering is observed.²⁸ Therefore, it is evident that the spatial spin modulation depends strongly on the electronic state of the doped carriers and/or the spin state of the undoped antiferromagnetic host. Thus any theoretical interpretation of the obtained doping dependence of the spatial spin modulation shown in Fig. 7 must take into account possible crossover behavior in the nature of the doped carriers.

B. Doping dependence of peak width

Since the crystallographic quality of all of our crystals is similar, the variation of the dynamical q -space broadening of the incommensurate peaks may be interpreted as an inherent property of this system. Figure 6 shows the doping dependence of κ_w from the underdoped to the overdoped region. One of the most interesting results is the anomalously narrow peak width observed for $x=0.12$; this may be related to the slight degradation of T_c observed for $\text{La}_{2-x}\text{Sr}_x\text{CuO}_4$ around $x=0.12$ as shown by the midpoint of T_c in Fig. 1(a). In fact, quite recently, an elastic incommensurate peak with a narrow q -width ($\kappa_w^{-1} > 100 \text{ \AA}$) which develops below 40 K, has been observed for $x=0.12$.²⁹ These phenomena are undoubtedly important in elucidating the microscopic mechanism for the degradation of superconductivity at this special doping, the so-called “ $\frac{1}{8}$ problem,” and in discussing the possibility of coexistence of superconductivity and long range antiferromagnetic order in the high- T_c cuprates.³⁰ However, at this stage more extensive measurements are necessary, so we do not discuss this subject further in this paper.

Except for this anomalous behavior of the width at $x = \frac{1}{8}$, κ_w depends at best weakly on x within the experimental errors for $0.06 \leq x \leq 0.18$, that is, from the underdoped through the optimal doping regions. Only for the highly overdoped region, $x \approx 0.25$, is significant q -space broadening of the low-energy spin fluctuations observed. Further, following our previous discussion of the possible crossover behavior of the carrier character from $O(2p)$ to $\text{Cu}(3d)$ type in the overdoped region, the degradation of the spin coherence length in the overdoped region may reflect the decrease of the magnetic interactions between the Cu spins due to $\text{Cu}(3d)$ -type carriers as already observed for the electron-doped materials $(\text{Nd,Pr})_{2-x}\text{Ce}_x\text{CuO}_4$.³¹

C. Linear relation between T_c and incommensurability

Perhaps the most surprising new result of this study is the linear relation between T_c and δ up to the optimal doping regime as shown in Fig. 10. Note, that the data plotted in Fig. 10 are completely free from any uncertainties connected with the doping level or oxygen stoichiometry in each sample. Furthermore, results from superconductors prepared by electrochemical oxygenation^{6,32} and heat treatment under high oxygen pressure fall on the same linear relation in Fig. 10.³² This empirical result connects directly the incommensurate

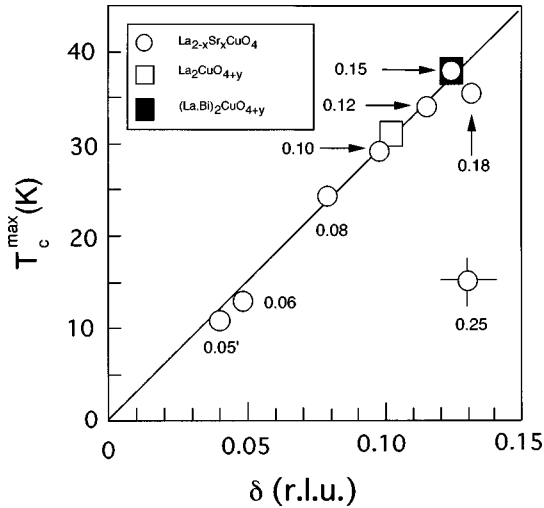


FIG. 10. δ as a function of onset temperature of T_c for stoichiometric $\text{La}_{2-x}\text{Sr}_x\text{CuO}_4$ (open circles), electrochemically oxygen-doped $\text{La}_2\text{CuO}_{4+y}$ (Ref. 6) (open square) or $(\text{La,Bi})_2\text{CuO}_{4+y}$ (Ref. 32) (closed square), and $\text{La}_{1.95}\text{Sr}_{0.05}\text{CuO}_4$ annealed under high O_2 pressure (Ref. 32) (closed circle).

spin correlations and the superconductivity. Concomitantly, this relation reconfirms the simultaneous appearance of both the superconductivity and the modulated spin correlations as is expected from Fig. 7. For the overdoped samples, however, the T_c values deviate from the δ - T_c relation. This implies the existence of an inherent mechanism to degrade the superconductivity in the overdoped region.

The nonzero incommensurability δ observed in the non-superconducting pair-broken samples might seem to be in conflict with the δ - T_c relation. Instead, it is important to emphasize that δ correlates with the upper limit of T_c at a given x , $T_c^{\text{max}}(x)$, although the superconducting transition itself, and hence T_c , is easily degraded by extrinsic pair-breaking effects such as oxygen vacancies or impurity doping in the CuO_2 planes.

V. SUMMARY AND CONCLUSIONS

In summary, we have performed systematic low-energy neutron-scattering measurements on float-zone-grown homogeneous single crystals of $\text{La}_{2-x}\text{Sr}_x\text{CuO}_4$ over a wide doping range between the lower and upper boundaries of the superconducting phase to study the spatially modulated dynamical spin correlations. Several new results have been obtained: (1) quantitative evidence for the sudden development of the modulated spin correlations beyond a critical doping value x_c for the superconducting phase, (2) a simple scaling of the maximum T_c at a given doping with the incommensurability δ up to the optimal doping, (3) robustness of δ against deoxygenation of a sample sufficient to destroy the superconductivity, (4) degradation of the dynamical spin coherence length in the overdoped region, (5) long-range dynamical coherence for $x \approx 0.12$.

Summarizing the discussions in the previous sections, we propose the following scenario for the doping dependence of T_c . In the underdoped region, both δ and $T_c^{\text{max}}(x)$ simultaneously appear at $x_c \approx 0.05$ and increase upon doping following an identical doping dependence. We speculate that the saturation of T_c occurs as a result of the saturation of the doped $\text{O}(2p)$ -type carrier number; we also speculate that the decrease of T_c in the overdoped region is caused by the shortening of the dynamical coherence length of the incommensurate spin fluctuations and this in turn may be caused by the decrease of the effective magnetic interactions upon a presumed $\text{Cu}(3d)$ -type carrier doping.

The data presented in this paper clearly represent a unique but formidable challenge for any theory of high- T_c superconductivity. Specifically, to identify the mechanism underlying high- T_c superconductivity one will undoubtedly need to understand the dynamical spin fluctuations. Further insight into this may be gained from studies of the electron-doped superconductors such as $\text{Nd}_{2-x}\text{Ce}_x\text{CuO}_4$; no signal from the spin fluctuations has as yet been detected in superconducting samples.²⁷ As in the case of $\text{YBa}_2\text{Cu}_3\text{O}_{7-y}$, the Fermi surface in the electron-doped materials is expected to be rotated by 45° compared with that in $\text{La}_{2-x}\text{Sr}_x\text{CuO}_4$,^{33,34} so that modulated spin correlations are not expected from a Fermi-surface nesting model, but would occur for example, in a charge-fluctuation model. Clarification of the similarity and dissimilarity of the spin fluctuations in the superconducting states of hole-doped and electron-doped systems should provide essential information on the electronic states of high- T_c superconductors and possibly on the mechanism itself. We note that incommensurate spin fluctuations seem to have been observed recently in underdoped $\text{YBa}_2\text{Cu}_3\text{O}_{7-y}$.³⁵

ACKNOWLEDGMENTS

We would like to thank V. J. Emery, H. Fukuyama, R. J. Gooding, H. Kamimura, K. Levin, P. Littlewood, and J. M. Tranquada for invaluable discussions of these results. We also would like to acknowledge M. Onodera, K. Nemoto, T. Toyoshima, and T. Takahashi for their assistance with the crystal growth, neutron scattering, and x-ray-diffraction measurements. The present work was supported by the U.S.-Japan Cooperative Neutron-Scattering Program. The work at Tohoku was supported by a Grant-in-Aid for Scientific Research on Priority Areas, ‘‘Science of High- T_c Superconductivity’’ (04240103), Ministry of Education, Science, Culture and Sports Japan, and by a Grant of the Science and Technology Agency, Japan. The research at MIT was supported by the NSF under Grant No. DMR97-04532 and by the MRSEC Program of the National Science Foundation under Award No. DMR94-00334. Work at Brookhaven National Laboratory was carried out under Contract No. DE-AC276CH00016, Division of Material Science, U.S. Department of Energy.

- ¹G. Shirane, R. J. Birgeneau, Y. Endoh, P. Gehring, M. A. Kastner, K. Kitazawa, H. Kojima, I. Tanaka, T. R. Thurston, and K. Yamada, *Phys. Rev. Lett.* **63**, 330 (1989).
- ²S.-W. Cheong, G. Aeppli, T. E. Mason, H. A. Mook, S. M. Hayden, P. C. Canfield, Z. Fisk, K. N. Klausen, and J. L. Martinez, *Phys. Rev. Lett.* **67**, 1791 (1991).
- ³T. E. Mason, G. Aeppli, S. M. Hayden, A. P. Ramirez, and H. A. Mook, *Phys. Rev. Lett.* **71**, 919 (1993).
- ⁴M. Matsuda, K. Yamada, Y. Endoh, T. R. Thurston, G. Shirane, R. J. Birgeneau, M. A. Kastner, I. Tanaka, and H. Kojima, *Phys. Rev. B* **49**, 6958 (1994).
- ⁵K. Yamada, S. Wakimoto, G. Shirane, C. H. Lee, M. A. Kastner, S. Hosoya, M. Greven, Y. Endoh, and R. J. Birgeneau, *Phys. Rev. Lett.* **75**, 1626 (1995).
- ⁶B. O. Wells, Y. S. Lee, M. A. Kastner, R. J. Christanson, R. J. Birgeneau, K. Yamada, Y. Endoh, and G. Shirane, *Science* **277**, 1067 (1997).
- ⁷N. Bulut, D. Hone, D. J. Scalapino, and N. E. Bickers, *Phys. Rev. Lett.* **64**, 2723 (1990); Q. Si, Y. Za, K. Levin, J. P. Lu, and J. H. Kim, *Phys. Rev. B* **47**, 9055 (1993); T. Tanamoto, H. Kohno, and H. Fukuyama, *J. Phys. Soc. Jpn.* **63**, 2739 (1994).
- ⁸S. A. Kivelson and V. J. Emery, in *Proceedings of Strongly Correlated Electronic Materials: The Los Alamos Symposium 1993*, edited by K. S. Bedell *et al.* (Addison-Wesley, Reading, MA, 1994), p. 619; V. J. Emery and S. A. Kivelson, *Physica C* **235-240**, 189 (1994).
- ⁹C. Nayak and F. Wilczek, *Phys. Rev. Lett.* **78**, 2465 (1997).
- ¹⁰A. Aharony, R. J. Birgeneau, A. Coniglio, M. A. Kastner, and H. E. Stanley, *Phys. Rev. Lett.* **60**, 1330 (1988); R. J. Gooding, N. M. Salem, R. J. Birgeneau, and F. C. Chou, *Phys. Rev. B* **55**, 6360 (1997).
- ¹¹C.-H. Lee *et al.* (unpublished).
- ¹²J. Wada, Master thesis, Tohoku University (in Japanese), 1996.
- ¹³S. Hosoya, C. H. Lee, S. Wakimoto, K. Yamada, and Y. Endoh, *Physica* **235-240**, 547 (1994).
- ¹⁴C. H. Lee, N. Kaneko, S. Wakimoto, J. Wada, S. Hosoya, K. Yamada, and Y. Endoh (unpublished).
- ¹⁵K. Yamada (unpublished).
- ¹⁶E. Takayama-Muromachi and D. E. Rice, *Physica C* **177**, 195 (1991).
- ¹⁷R. Yoshizaki, N. Kuroda, S. Nakamura, and N. Ishikawa, *Physica C* **199**, 143 (1992).
- ¹⁸K. Kurahashi, S. Wakimoto, C. H. Lee, K. Yamada, and S. Hosoya, *J. Phys. Soc. Jpn.* **65**, 3994 (1996).
- ¹⁹B. Keimer, N. Belk, R. J. Birgeneau, A. Cassanho, C. Y. Chen, M. Greven, M. A. Kastner, A. Aharony, Y. Endoh, R. W. Erwin, and G. Shirane, *Phys. Rev. B* **46**, 14 034 (1992).
- ²⁰T. Arakawa, Master thesis, Kobe University (in Japanese), 1997.
- ²¹M. Matsuda, R. J. Birgeneau, H. Chou, Y. Endoh, Y. Hidaka, M. A. Kastner, K. Nakajima, G. Shirane, T. R. Thurston, and K. Yamada, *J. Phys. Soc. Jpn.* **62**, 1702 (1993).
- ²²K. Hirota, K. Yamada, I. Tanaka, and Y. Kojima (unpublished).
- ²³J. B. Torrance, Y. Tokura, A. I. Nazzari, A. Bezing, T. C. Huang, and S. S. P. Parkin, *Phys. Rev. Lett.* **61**, 1127 (1988).
- ²⁴H. Kamimura and Suma, *J. Phys. Soc. Jpn.* **62**, 3368 (1993).
- ²⁵F. Onufrieva, S. Petit, and Y. Sidis, *Physica C* **266**, 11 (1996).
- ²⁶S. Uchida, T. Ido, H. Takagi, T. Arima, Y. Tokura, and S. Tajima, *Phys. Rev. B* **43**, 7942 (1991). We borrowed the original data of N_{eff} at 1.2 eV from Professor S. Uchida.
- ²⁷M. Matsuda, K. Yamada, K. Kakurai, H. Kadowaki, T. R. Thurston, Y. Endoh, Y. Hidaka, R. J. Birgeneau, M. A. Kastner, P. M. Gehring, A. H. Moudden, and G. Shirane, *Phys. Rev. B* **42**, 10 098 (1990).
- ²⁸H. Yoshizawa (private communication).
- ²⁹T. Suzuki, T. Fukase, and K. Yamada (unpublished).
- ³⁰J. M. Tranquada, B. J. Sternlieb, J. D. Axe, Y. Nakamura, and S. Uchida, *Nature (London)* **375**, 561 (1995).
- ³¹T. R. Thurston, M. Matsuda, K. Kakurai, K. Yamada, Y. Endoh, R. J. Birgeneau, P. M. Gehring, Y. Hidaka, M. A. Kastner, T. Murakami, and G. Shirane, *Phys. Rev. Lett.* **65**, 263 (1990).
- ³²S. Wakimoto (private communication).
- ³³D. M. King, Z. X. Shen, D. S. Dessau, B. O. Wells, W. E. Spicer, A. J. Arko, D. S. Marshall, J. DiCarlo, A. G. Loeser, C. H. Loser, C. H. Park, E. R. Ratner, J. L. Peng, Z. Y. Li, and R. L. Greene, *Phys. Rev. Lett.* **70**, 3159 (1993).
- ³⁴R. O. Anderson, R. Claessen, J. W. Allen, C. G. Olson, C. Janowitz, L. Z. Liu, J. H. Park, M. B. Maple, Y. Dalichaouch, M. C. deAndrade, R. F. Jardim, E. A. Early, S. J. Oh, and W. P. Ellis, *Phys. Rev. Lett.* **70**, 3163 (1993).
- ³⁵P. Dai, H. A. Mook, and F. Dogon, *Phys. Rev. Lett.* (to be published).
- ³⁶H. Takagi, R. J. Cava, M. Marezio, B. Batlogg, J. J. Krajewski, W. F. Peck Jr., P. Bordet, and D. E. Cox, *Phys. Rev. Lett.* **68**, 3777 (1992).
- ³⁷T. Nagano, Y. Tomioka, Y. Nakayama, K. Kishio, and K. Kitazawa, *Phys. Rev. B* **48**, 9689 (1993).